VĚDECKÉ SPISY VYSOKÉHO UČENÍ TECHNICKÉHO V BRNĚ

Edice PhD Thesis, sv. 446

ISSN 1213-4198

Ing. Zdenka Sant

Mechanical Properties of Thoracolumbar and Lumbar Spine Fixation Device

BRNO UNIVERSITY OF TECHNOLOGY
FACULTY OF MECHANICAL ENGINEERING
Institute of Solid Mechanics, Mechatronics and Biomechanics

Ing. Zdenka Sant

MECHANICAL PROPERTIES OF THORACOLUMBAR AND LUMBAR SPINE FIXATION DEVICE

Mechanické vlastnosti hrudního a bederního páteřního fixátoru

SHORT VERSION OF Ph.D. THESIS

Study field: Engineering Mechanics
Supervisor: Ing. Zdeněk Florian, CSc.
Opponents: prof. Ing. Dušan Šimšík, Ph.D.
prof. Ing. Přemysl Janíček, Ph.D.
MUDr. Ján Kočiš, Ph.D.
Presentation date: 13. 12. 2007

Key words
Biomechanics, posterior spinal fixation, spinal segment, fusion, finite element analysis

Klíčová slova
Biomechanika, posteriorní páteřní fixátor, páteřní segment, fúze, metoda konečných prvků

Storing place of the thesis
Oddělení pro vědu a výzkum
FSI VUT v Brně, Technická 2896/2, Brno, 616 69

ISBN 978-80-214-3586-5
ISSN 1213-4198

CONTENT

1 INTRODUCTION

The task to evaluate the spinal strength has started during WWII, and is in progress even today. The major interest of the research is to help to understand and improve the treatment by means of design of new medical devices used to treat various spinal disorders or trauma. The new knowledge is achieved either via experiments in vivo or in vitro or by means of analytical or numerical computation.

The musculo–skeletal system formed by bones, muscles, tendons, ligaments and other soft tissues represents very complex biomechanical system. The spine, formed by 24 vertebrae connected via intervertebral discs, and fused sacral vertebrae, is the largest part of the skeleton to which all limbs are attached. It provides mobility together with load bearing ability. It has three fundamental biomechanical functions:

- Protection of the spinal cord and the nerve roots coming out
- Ability to transfer the load to the pelvis
- Enabling movement and ensuring the stability

Large number of people is experiencing low back pain (LBP) problems caused by intervertebral damage that affects the redistribution of load transferred through the segment and might initiate collapse of vertebral body. LBP is associated as well with trauma caused due to spinal overload because of either traffic accident or fall.

One of the most reliable ways to reduce LBP is to fuse the spinal segment. Spinal fusion is a surgical technique in which one or more of the spine vertebrae are fused so that the relative motion no longer occurs between them. Spinal fusion rate is affected by the mechanical stability of the involved segment therefore to increase fusion rates the internal posterior/anterior spinal fixation device is used. The non-union of fusion mass reaches 10–15% especially when hardware loosening or failure occurs.[1] Complications that could prohibit complete union of the segment include implant failure either due to fracture or migration, and fusion problems related to pseudarthrosis and non–union. This indicates that more studies are required to gain better knowledge that would give us the ability to quantify patient's response to treatment.

2 ANALYSIS OF THE PROBLEM SITUATION

The desired complete fusion would take place if the stability of spinal segment were satisfied together with dynamic transfer of the load through the segment to enhance the fusion process that is highly influenced by systematic factors, fusion enhancers, and local factors. The local factors, mainly the mechanical stability and loading character can be influenced by means of fixation device selection.[2] The fusion process can be described as deposition on new bone and remodelling of the present bone surrounding the implant. Since the formation of new bone obeys Wolff's law, thus the implant design has direct influence on the fusion.

2.1 PEDICLE SCREW FIXATION DEVICE

The manufacturing company tests the implant prior to clinical tests and mass production. The comparison of mechanical properties of various fixation devices is very difficult since the standards were not available until ASTM F 2267–04 “Standard Test Method for Measuring Load Induced Subsidence of an Intervertebral Body Fusion Device Under Static Axial Compression” was approved in late 2004. The results depicting the flexural rigidity/stiffness, bending strength and the fatigue of the fixation device are available in the literature [3], [4] without possibility to compare various constructs due to differences in procedure and loading. The local strain at the bone – implant interface represents another attribute that could help to predict the outcome of fusion process. Unfortunately, this information is not provided by manufacturers thus, it is difficult to foresee problems that could lead to non–union.

3 THE AIM OF THE THESIS AND METHODOLOGY OF SOLUTION

During surgical treatment of LBP the AO USS, implants are used mainly posterior in St. Luke’s Hospital, Malta. The applied fixation device remains in its position even after the complete fusion is reached. The interaction between fixation device and the spinal segment influences the fusion process, and determines the success of the surgery. There are published works comparing different implants from the point of their stability, strength, and fatigue but no works determined the stress/strain distribution as it will developed as a biomechanical feedback to loads simulating the affect of various activities on the segment stabilized with AO USS spinal fixation device. All this formed the background to formulation of the aim of the thesis as to:

Investigate the stress and strain distribution induced due to transfer of the load through the spinal segment with inserted spinal implant AO USS and the biomechanical feedback at the bone – implant interface, and at the fusion mass interface by means of computational simulation. Further to this computation the comparison between the single oval shaped megacage fusion mass and two cylindrical fusion masses supporting the vertebral body will be carried out.

The problem is going to be solved by means of computational modelling using finite element analysis with the following tasks:

1) Create computational model consisting of a composition of bodies representing vertebra, AO USS spinal fixation device for trauma made up of pedicle screw, side–opening sleeve, nut, and rod inserted into a vertebra via pedicle and completed with
    a) one or
    b) two fusion masses

2) Provide the analysis of stress and strain distribution on the interface between bone – fixation device, and bone – fusion mass due to applied load representing various positions of the spine for both versions a) and b). Finally, compare the effect of the two fusion masses on the stress and strain distribution within the vertebra, mainly at the fusion site.

4 RESEARCH ADVANCES IN LUMBAR SPINE

The biomechanical studies are targeting the quantification of spinal loads and movements, analysing the load distributions and injury mechanisms with prospect to develop the best therapeutic interventions. The interaction between intervertebral disc and adjacent vertebrae, development of medical devices, prosthetics and tissue–engineered discs, and spinal function assessment during rehabilitation are the three main research areas in lumbar spine biomechanics. The problems of interaction include the contribution of cancellous and cortical bone to load transfer, the function and properties of intervertebral disc, the contribution of facet join to load bearing function, the properties of ligaments and contribution of muscles to the complex function of the lumbar spine, and the magnitude of load transferred through the intervertebral disc and facet articular processes [4], [5], [6], [7], [8], [9], [10], [11], [21], [22], [23], [24], [25], [26], [27], [28], [29], [30], [31], [32], [33], [34], [40], [93]. The development of medical fixation devices and prosthetics and its use to investigate the spinal load in vivo [29], [30]. The spinal functionality includes the kinematics of the spine, evaluation of the range of motion, relation between the position of instantaneous axis of rotation and the stability of the spine, [4], [5], [7], [12], [13], [14], [15], [16], [17], [18], [19], [20], [22], [27], [41], [43], [45]. The degenerative process accompanying the ageing causes changes in the form and composition of spinal tissues causing internal disruption of intervertebral disc or the stress shielding [2], [5], [47], [48], [49]. Mechanism of spinal injury are discussed in works [3], [19], [51], [52], [53], [54], [55]. Due to complexity of the problems and inability to provide large amount of tests in vivo there are number of papers discussing experimental, and computational simulations of the spine behaviour [27], [32], [35], [36], [37], [38], [39], [42], [44], [45], [46], [71], [72], [82], [83].

The material properties of cortical and cancellous bone tissue and the influence of various factors on the properties, together with tests methods are presented in [19], [40], [50], [56], [57], [58], [59], [60], [61], [62], [63], [64], [65], [66], [67], [68], [69], [70], [71], [72], [73], [74], [75], [76], [77], [78], [79], [80], [81], [84], [85], [86].

Surgical implants, their properties, and factors influencing the success of the surgery are discussed in number of papers related to mechanical properties, geometry factors, surface treatments, and tests of surgical implants [2], [3], [4], [54], [87], [88], [89], [90], [91], [92], [93], [94], [95], [96].

5 COMPUTATIONAL MODEL

The goal is solved by means of computational modelling and use of finite elements method that is developed from variation principles of mechanics. Due to the complexity of the geometry and the whole system, a 3D solid model will be created in finite element software package ANSYS, high university version with 128000 nodes limit, and solved as a direct task. The real system of two vertebrae and implant bridging the traumatic vertebra was modelled with assumption of symmetry with respect to medial and transverse plane. One quarter of the system was created consisting of half of the vertebra L2 with pedicle screw inserted via pedicle and fastened by means of nut securing the sleeve that locks the rod in the position. The task includes contacts between parts of the implant that are involved in the load transfer.

5.1 MODEL OF GEOMETRY

Creation of computational model consists of three steps: creation of geometry, application of boundary conditions, and loading of the model.

During the first step the geometry model of vertebra was created based on the data of vertebra geometry that were achieved by means of direct measurement of vertebra outline from the wooden model.

The geometry of USS spinal fixation device was obtained from manufacturing company Mathys–Medical after the confidential agreement was signed. The geometry model of fixation device omits some of the details such as the hole for manipulation with the screw, grating of the edges for better grip with the rod, and bone. These features play insignificant role in the task as outlined above.

The side–opening screw was modelled as a sequence of discs attached together while the profile of each disc varies according to the position on the screw axis as the thread varies its profile in reality. The outer thread on the screw head was omitted from the model. In fact, the screw and nut assembly was considered as a single element of the system. The sleeve and the nut were modelled according to the original drawings received from the company except for the thread as mentioned earlier.

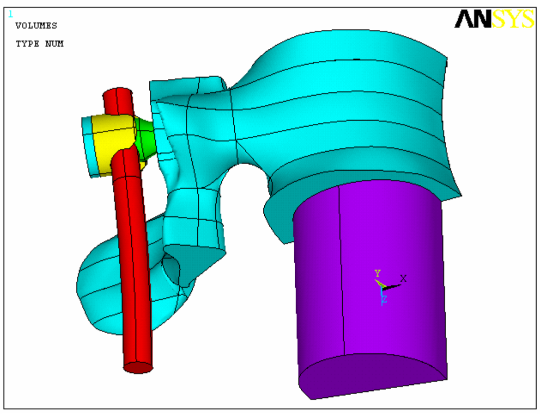

Fig. 5-1: *Model M6 – single cage*

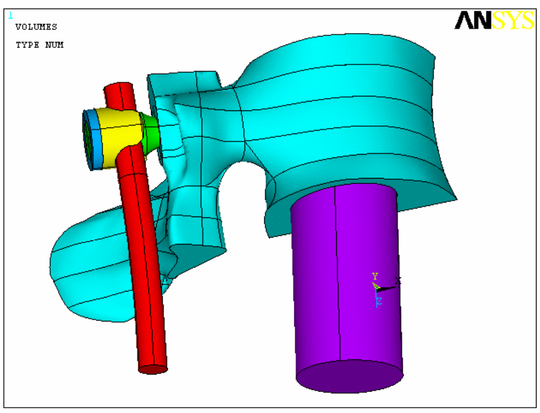

Fig. 5-2: *Model M7 – two cages*

The fusion mass that is created in two different models M6 and M7 as a half of the single ovalshaped cement column and as the small circular column respectively, is finalizing the whole system of vertebrae and implant.

5.1.1 Mesh generation

During the discretization, known as generation of the mesh, the basic rule of continuity of the solid model was observed so no overlaps between nodes would occur and connectivity between them would be satisfied.
Type of element used to mesh each item of the system is listed in Table 1.

5.1.2 Model of load transfer

The numbers of contact regions were identified and contact pairs were created with Surface – to – Surface contact type. The standard condition of contact behaviour was set for all pairs together with penalty contact algorithm.
The normal penalty stiffness and penetration tolerance was set for each contact and tuned to the reach convergence criteria.
The contact at the thread screw – bone interface was not modelled due to hardware and software limit. Therefore, the behaviour at this region was controlled via coupling equations.

5.2 MODEL OF MATERIAL

The vertebra model consists of two types of bone – cortical and cancellous bone. The bone is modelled as a continuous linearly elastic material in both cases. This assumption is reasonable in all static investigations or non-impact conditions of

Material properties of the model components				
Component	material	Young's modulus E [MPa]	Poisson's ratio μ [–]	Element Type
vertebra	cortical bone	14100	0.3	SHELL93
	cancellous bone	160	0.3	SOLID95
	endplate	600	0.3	SHELL93
screw	titanium alloy	105000	0.31	SOLID45
	titanium alloy	105000	0.31	SOLID95
sleeve	titanium alloy	105000	0.31	SOLID95
nut	titanium alloy	110000	0.31	SOLID45
rod	titan hard	105000	0.342	SOLID45
fusion mass	cement	2500	0.3	SOLID45

Table 1: *Model attributes*

loading. The cortical bone is covering all external areas of the vertebra except of the superior and inferior endplates. The cortical bone thickness was assumed 1 mm. The endplate thickness of 1 mm was assigned isotropic material properties thus, modelling the cartilage covered by subchondral bone as continuum.

The material properties for USS implant were found from the literature based on information received from Mathys-Medical Company. Screw, nut and sleeve material is $TiAl_6Nb_7$ with tensile strength 900 MPa and stretch 10% for screw and sleeve while nut has tensile strength 1100 MPa and stretch of 10%. The rod material is 'TiCP hart' with tensile strength of 800-900 MPa. The fusion mass was made of cement without the cage consideration.

5.3 BOUNDARY CONDITIONS

The boundary conditions prescribed to the model have to specify the model behaviour in the space. Due to the assumption of ideal symmetry along the median plane together with symmetry with respect to transverse plane is imposing the boundary symmetry condition to be applied. All degrees of freedom were taken away for all nodes on the median plane and on the transverse plane passing through the mid – span of the rod.

5.4 MODEL OF THE LOAD

The validated data, based on the computation and tuned according to measured data that were published recently [27] were used to load vertebra while the affect of ligamentous structures and muscles on the spine behaviour is passive. The data were applied to the model through the node associated with bonded contact pair on top of the vertebra, to simulate the upright and flexed position with or without carrying load of 180 N in hands. The position of the node corresponds to the midplane of the adjacent intervertebral disc, where the intradiscal pressure was measured and corresponding forces were computed. The vertebra was loaded on the superior endplate with forces and moment corresponding to load at L1 - L2 intervertebral disc. Different load models were not considered because the contribution of the abdominal and thoracic cavity pressure to load bearing ability is still not understood. As well as load by means of displacement prescribed to the structure would involve the affect of ligamentous structures including the muscle contribution, and abdominal pressure.

The task was solved as a non-linear problem using Newton-Raphson numerical method, running on PC with following configuration:

Intel P4, RAM 0.9 GB, HDD 120 GB, OS Windows XP.

6 RESULTS SUMMARY

The computation was done for two models M6 and M7, each model loaded with three different flexion angles with/without carrying load of 180 N. Thus twelve sets of results were analysed and the two models were compared.

6.1 STABILITY OF THE SPINE WITH FIXATION DEVICE

The stability of the spine can be evaluated based on the position of instantaneous axis of rotation (IAR). The position of IAR reflects the spine activity thus for various positions of the spine the point that experiences zero movement can be identified and compared with general location for IAR. The position of IAR in traumatic spine varies according to the disruption of the spinal column. Thus, the reverse process of establishing stability can use the same principle of IAR.

Model M6 Model M7

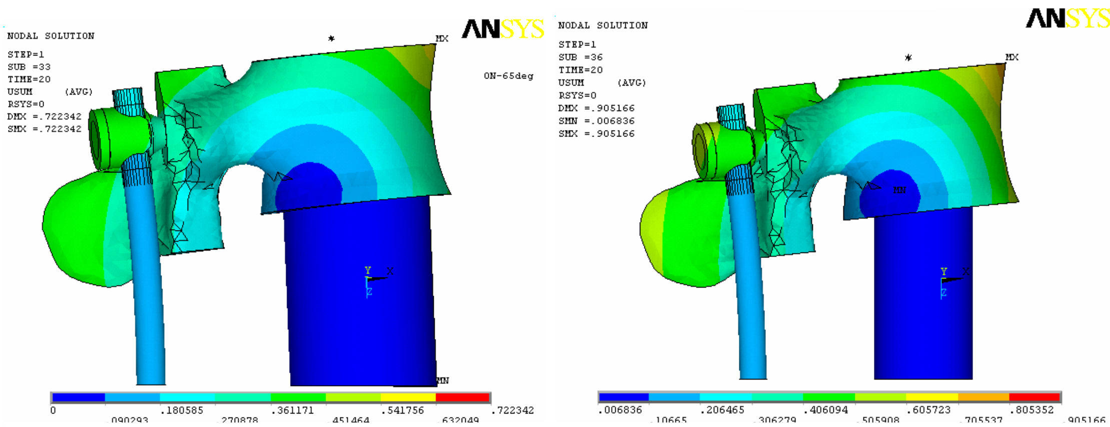

Fig. 6-1: *Comparisson of the IAR position set up in M6 and M7, under the spine flexion65^{0} without carrying load.*

6.2 THE FUSION SITE ANALYSIS

The main aspect of fusion site evaluation is the ability to promote fusion that is closely related to bone deposition and bone remodelling. The two important quantities that have to be investigated are the relative motion between the vertebra and fusion mass and the principal stress/strain developed at the fusion site due to applied load.

6.2.1 The strain at the fusion site

Formation of new bone takes place in two ways. The first way involves direct remodelling under the tissue strain that would not exceed 2%. The second way of the healing process comprises of a combination of intramembranous and endochondral ossification while the tissue strain reaches 2% to 10%, according to the healing theory. Strain above 10% results in fibrous tissue formation and ultimately in non–union if the tissue strain reaches 100%.[97]

Analysis of model M6

The maximum strain ε_1 due to compressive load reached 0.010555 at the anterior site of the vertebral body under the flexion of 65^0 while carrying load 180 N. In case of the same flexion of 65^0 without any load applied, the strain reached 7.37E-03 at the anterior site of the vertebral body.

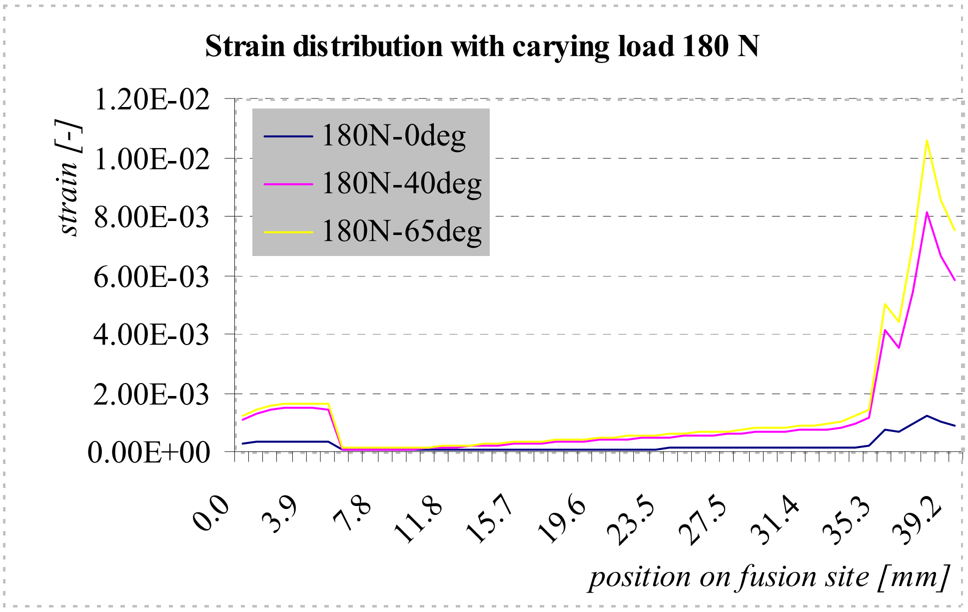

Fig. 6-2: *Strain ε_1 distribution at the fusion site on model M6*

The minimum strain reached ε_3 = -0.00028452 and ε_3 = -0.000046824, due to spine flexion by 65^0 while carrying load and without load respectively.

Analysis of model M7

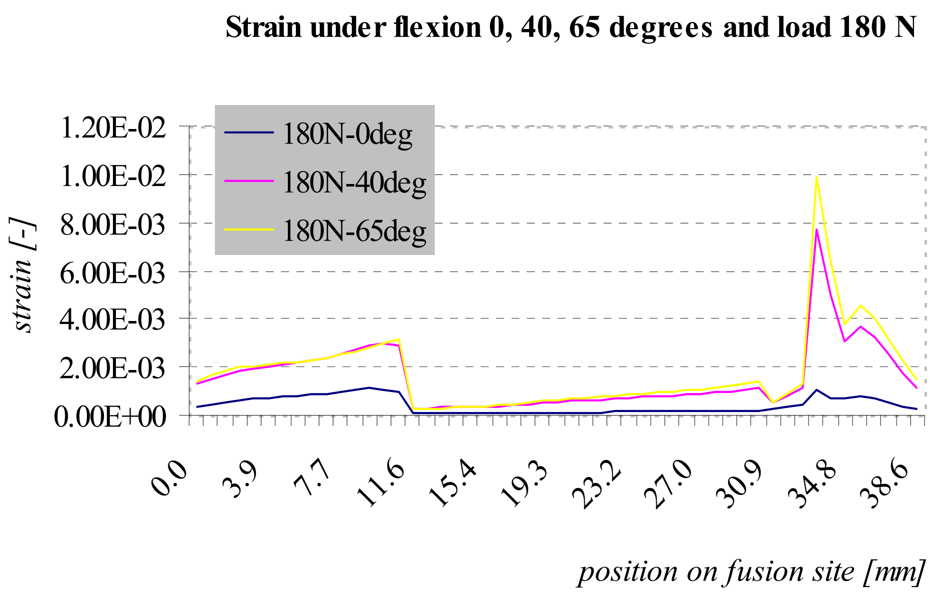

Fig. 6-3: *Strain ε_1 distribution at the fusion site on model M7*

The maximum strain in model M7 without carrying any load reached ε_1 = 0.0066564 while flexed by 65^0 and minimal strain ε_3 = -0.042826 due to compressive load under the same flexion of 65^0 without carrying load. Both extreme values appeared at anterior site of the vertebral body.

The maximum strain at flexion 65^0 carrying 180 N loads reached ε_1 = 0.0098829 and the minimum strain reached ε_3 = -0.061819 at the anterior part of the vertebral body.

6.2.2 The relative motion at the fusion site

Another factor that influences the successful fusion is the relative motion between fusion mass and the bone. 'Micromotion as little as 100 to 500 µm between bone and implant is sufficient to inhibit bone ingrowth and result in a fibrous membrane forming between the two, resulting in a mechanically unstable implant.'[58] Due to excessive motion at the fusion site the callus cannot be transformed into a solid mineralised bone.

Analysis of the relative motion between vertebra and fusion mass were done along the path P1 passing through the four nodes on the sagittal plane of the vertebra and fusion mass for model M6, and path P2 for model M7, passing through the four common nodes on the fusion site of the vertebra and fusion mass that is slightly tilted with respect to the median plane.

Analysis of model M6

The relative motion between vertebra and fusion mass evaluated on the path P1 reaches the maximum of *0.05881 mm* during the flexion 65^0 without carrying load. The minimal relative motion of *0.000521 mm* occurs again during the flexion 65^0 while carrying load of 180 N.

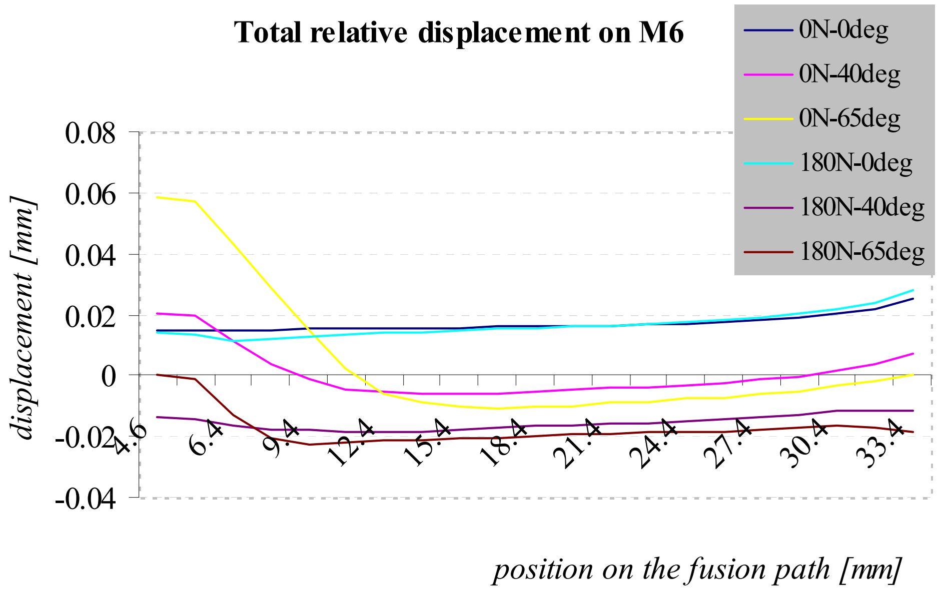

Fig. 6-4: *The distribution of total relative displacement along the path P1 on M6*

Analysis of model M7

The relative motion between vertebra and the fusion mass was evaluated on the path P2 passing through the common nodes at the fusion site of the vertebra and fusion mass. The relative motion between vertebra and fusion mass is negligible along the path reaching zero micromotion at the centre of the fusion mass. The highest relative motion is recorded at the periphery of the fusion mass and does not exceeds *0.06 mm* and *0.05 mm* for flexion without and with carrying load 180 N respectively.

6.2.3 The stress at the fusion site

Analysis of model M6

The stress distribution was mapped on the fusion path P3 created by two nodes. One node lays on the sagittal plane while the other is positioned at the first node away from sagittal plane to record the highest stresses that occur at the location very close to sagittal plane.

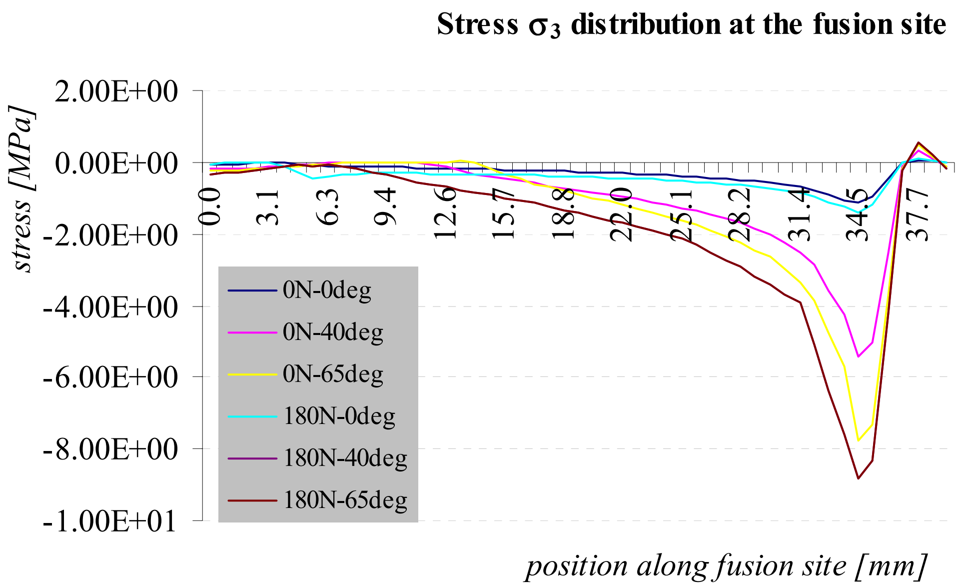

Fig. 6-5: *Stress distribution at the fusion site on M6*

Distribution of the third principal stress is important for bone remodelling process and orientation of trabeculae during mineralization process. Regions that are exposed to tensile stresses that are represented mainly by first principal stress are more likely to have trouble during the fusion process.

The maximum stress σ_3 occurred at the anterior portion of vertebral body where the fusion mass is in the contact with the bone, under the flexion 65^0 reaching 7.75 MPa and 8.85 MPa in compression without carrying load and 180 N load respectively.

Analysis of model M7

The stress distribution was mapped on the fusion path P4 created in a way that extreme stress can be recorded.

The location of extreme stress is positioned on the anterior site of the vertebra at the location of the vertebra edge contact with fusion mass. It corresponds to the position of the maximum stress on the model M6. The highest compressive stress reached 13.41 MPa and 9.26 MPa under the flexion of 65^0 carrying 180 N and without load respectively.

6.3 ANALYSIS OF THE SCREW – IMPLANT INTERFACE

The pedicle screw is part of the bypassing construct through which the load is redirected from the superior vertebra via posterior screw – rod system to the inferior vertebra. Excessive stress at the interface would cause micro damage to trabeculae at that location and consequently results in implant loosening.

The screw is exposed to the bending stress. Once again the third and first principal stresses are of the importance.

6.3.1 Model M6 analysis

The maximum compressive stress σ_3 reaching the value of 2.58 MPa is produce under the spine flexion of 65^0 while carrying 180 N loads. The maximum tensile stress occurs again during the flexion of 65^0 reaching 0.58 MPa. The minimum

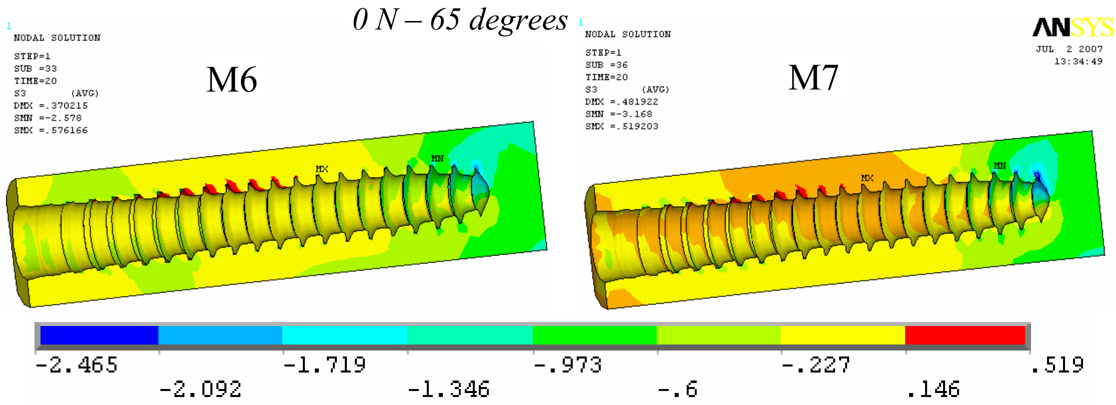

Fig. 6-6: *Comparison between model M6 and model M7 distribution of σ_3 under 65^0 flexion angle without carrying load*

tensile stress σ_3 is reaching 0.08 MPa occurs during upright straight standing position. The position of maximum stress varies according to the angle of flexion. The minimum stress is located at the third screw thread disc for all flexions.

6.3.2 Model M7 analysis

The maximum compressive stress σ_3 reached 3.17 MPa under the spine flexion of 65^0 while carrying 180 N loads. The maximum tensile stress under the same condition reached 0.52 MPa. The minimum tensile stress occured during upright straight standing position and reached 0.07 MPa. The minimum stress is located at the third screw thread disc for all flexions while the position of maximum stress varies according to the angle of flexion.

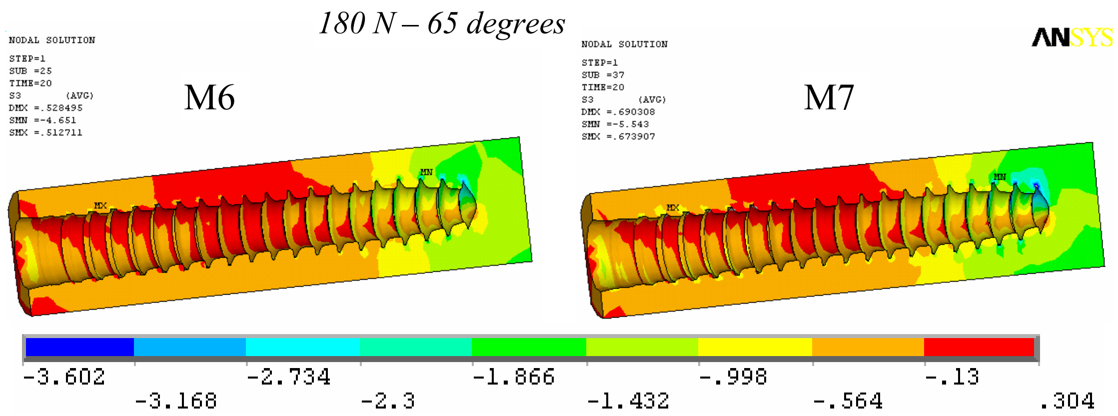

Fig. 6-7: *Comparison between model M6 and model M7 distribution of σ_3 under flexion 65^0 while carrying load180 N*

6.3.3 Analysis of the screw

The excessive stresses within the implant may cause failure of that component, which may result in failure of the whole construct prior to successful fusion. The pedicle screw is exposed to bending stresses. The most critical case under the flexion 65^0 and the load 180 N, will give the rise to bending stresses reaching 89 MPa and 126.54 MPa in model M6 and M7 respectively. Bending stresses don't represent the maximum stress that develops in the screw. The maximum stress occurs in a very small region where the contact between the screw and the rod takes place. The point contact develops stress up to 403.23 MPa and 319.7 MPa in model M7 and M6 respectively. These stresses are below the yield tensile stress of 790 MPa for given screw material. Therefore, it can be concluded that the yield stress is not exceeded in any of the computed flexion positions.

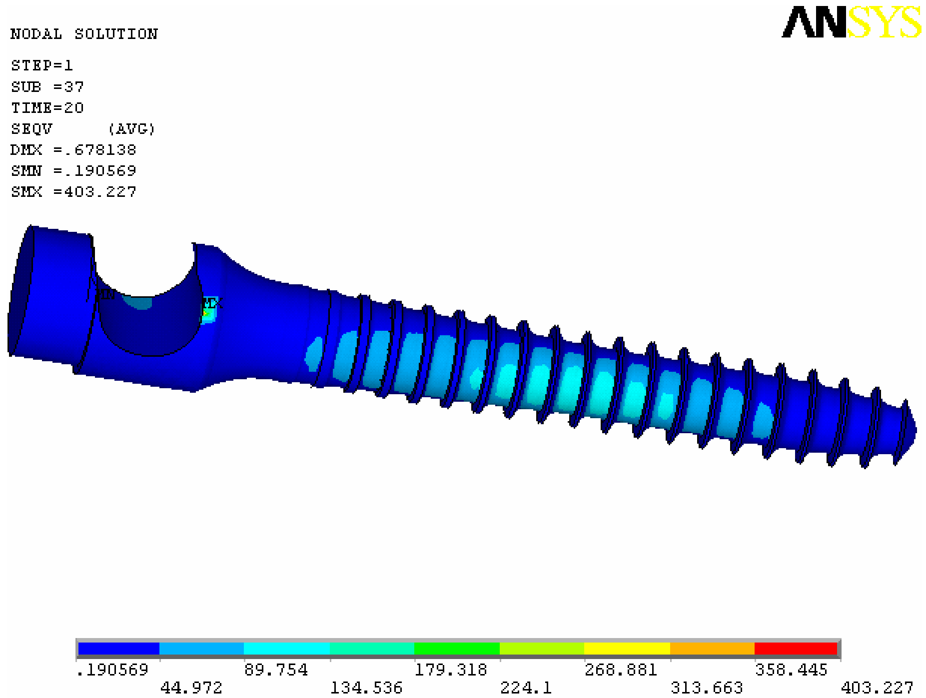

Fig. 6-8: *Distribution of von Misses stress on the screw in M7*

6.4 ANALYSIS OF THE ROD

The connecting rod plays very important role in bridging construct. It is exposed to high compressive stresses that could lead to buckling failure of the rod.

6.4.1 Displacement analysis

The maximum displacement that occurred due to different load conditions was evaluated with respect coordinate system associated with the model. The maximum displacement in the direction of x-axis, posterior direction in the lateral plane, reached 0.39613 mm in the model M6 and occurred at the superior top of the rod while loaded with 65^0 flexion, and carrying 180 N loads.

The maximum displacement in y-direction, lateral direction in frontal plane, reached value 0.17149 mm that occurred in the caudal direction on the plane where boundary condition of symmetry were prescribed to the rod while loaded by 65^0 flexion and carrying 180 N load applied to model M7.

The maximum displacement in z-direction, inferior direction in the lateral plane, reached 0.003062 mm at the inferior end of the rod while model M7 was loaded with 65^0 flexion and 180 N load.

The maximum total displacement occurred in model M7 at the superior end of the rod under 65^0 flexion and load 180 N.

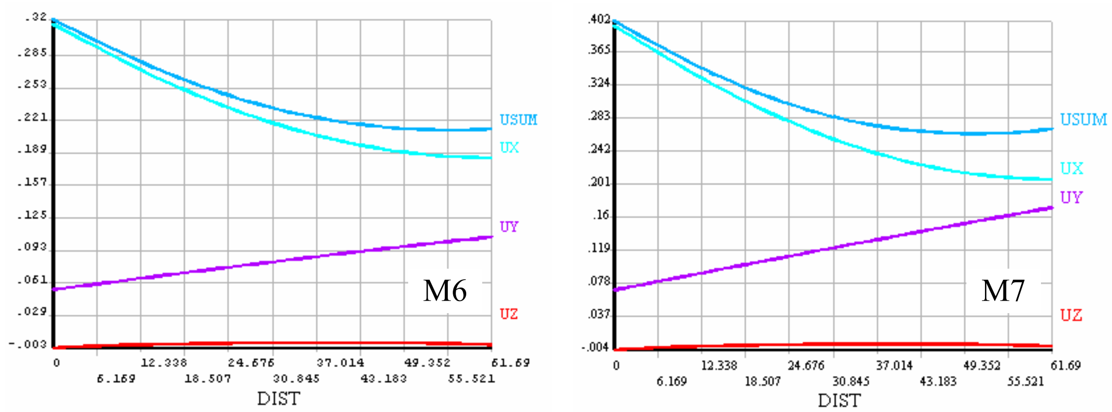

Fig. 6-9: The influence of fusion mass shape on displacement under 65 degree flexion, carrying180N load

6.4.2 Stress analysis

The maximum von Misses stress occurred at the rod's plane of symmetry reaching 31.46 MPa in model M7 while carrying load 180 N while the spine is flexed by 65^0. The yield stress of the rod's material reaches 790 MPa and therefore there is no potential danger that the stress would be exceeded for any of the simulated tasks.

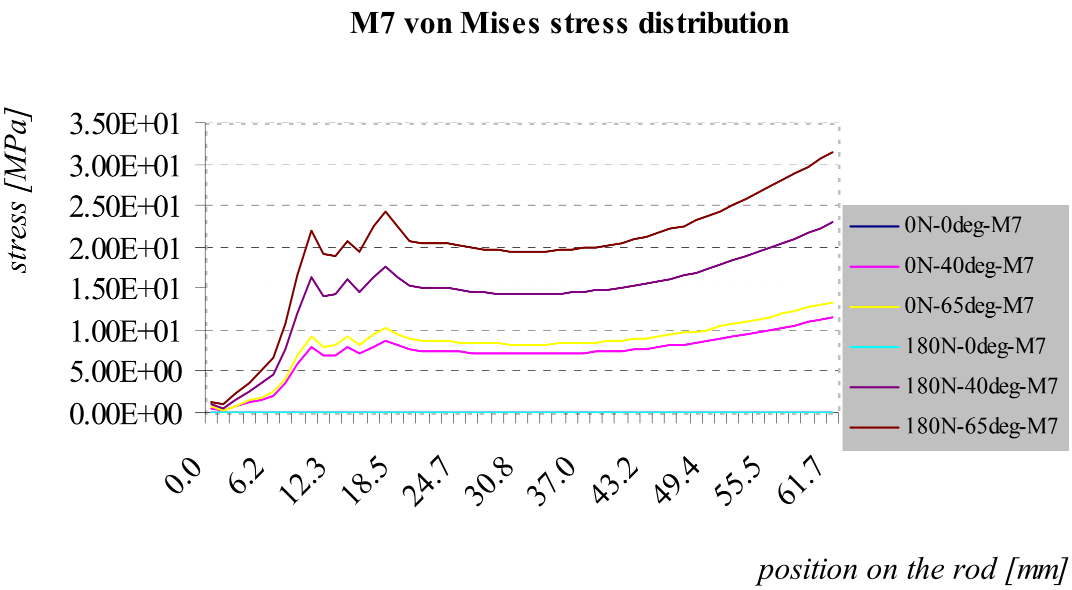

***Fig. 6-10:** The influence of fusion mass shape on stress distribution under various flexion positions and load*

7 CONCLUSION

The task, to model and simulate load transfer through the spinal segment and surgical fixation device inserted via pedicle screw completed with the fusion mass, was accomplished. The computation was run successfully and results indicated following outcomes:

1. The two small circular fusion masses give rise to the higher stresses developed at the fusion site reaching 13.41 MPa in compression. On the other hand this set – up results in minimum relative motion between fusion mass and vertebra. The minimum relative displacement is equal to zero at the centre of the fusion mass, and the maximum strain of 0.0098829 that does not exceed 2%, proposes the first mode of bone healing process.

Stresses developed within the fusion site might differ in reality and further analysis are required with respect to cage model as well as material model of the bone at the region where contact between the cage and bone occurs.

2. The maximum compressive stress developed at the bone – fusion mass interface in model M6 reached 8.85 MPa while spine was flexed by 65^0 with load of 180 N applied. The relative motion in model M6 reached its maximum value of 0.05881 mm while the spine was in the same position without carrying load. This magnitude of micromotion that does not exceed 0.5 mm promotes the fusion process. The maximum strain in model M6 reached 0.010555 while spine was flexed by 65^0 carrying 180 N loads. Therefore it can be concluded that the fusion is going to be promoted. This is based on the strain developed at the interface and relative motion at the same region, The healing process would follow the second mode when a combination of intramembranous and endochondral ossification is taking part in the process.

3. The maximum compressive stress developed within the pedicle screw – bone interface reached the highest value while the spin was flexed by 65^0 while carrying 180 N load. The value of maximum stress reached 3.17 MPa in model M7 and
2.58 N in model M6. These values should be compared to some clinical data that are not available at the present time. "The physiological stress levels for bone are generally below 1MPa." [59] This fact can't be used to compare computed values and the clinical observation since the bone material model was based on bone as a continuum with isotropic properties. It is well known that cancellous bone helps to redistribute the stress from cortical bone in more uniform manner. Therefore the stresses within the cancellous bone might be reduced. The assessment of the bone stresses based on the single trabecula failure stress does to lead to correct conclusion neither since the strength of the single trabecula is measured along the longitudinal axis thus it is not possible to extrapolate to the strength of the bone as a continuum.

4. Analysis of the rod revealed that the largest movement of the rod takes place in model M7 under the flexion of 65^0 carrying 180 N loads. It occurs on the superior part of the rod where the total displacement due to vertebra movement together with deformation reaches 0.4022 mm. The highest von Misses stress with magnitude of 31.46 MPa develops on the inferior site of the rod in transverse plane that corresponds to the second plane of symmetry, under the same load conditions. The second highest stress occurs at the superior part of the rod at the location of the contact with the sleeve/screw. The stress at this location does not exceed 2.5 MPa in model M7.

5. The screw analysis revealed that the highest bending stress develops in model M7 under the flexion of 65^0 while carrying 180 N load. It reached 126.54 MPa and developed at the mid – span of threaded part of the screw. This stress is not the highest stress developed in the screw. The highest von Misses stress on the screw reaches up to 403.23 MPa at the contact region under the same load condition. Due to the complex motion of the screw and vertebra with respect to the rod and deformations that develop in the whole system, the contact region is reduced to an edge contact between sleeve and the rod that would give the rise of such a high stress.

6. The highest von Misses stress developed in the sleeve of model M7 is due to flexion 65^0 while carrying 180 N load and reaches 175.53 MPa at the region of contact with the rod.

The comparison of the two fusion masses showed differences in the healing fusion process based mainly on the micromotion and strain developed at the site. In both cases, the fusion is promoted but the quality of bone would differ.

The highest stresses 403.23 MPa is developed within the implant made of titanium alloy with the yield stress reaching 790 MPa. The comparison of the stress developed within the implant and the yield stress gives the answer about possibility of implant failure due to plastic deformation. Therefore, all stresses that develop in the implant due to spine flexion 0, 40, and 65^0 fall below yield limit and the yield stress is not going to be exceeded for any of the mentioned load conditions.

All results related to fusion site or the bone – implant interface should be analysed very carefully while keeping in mind the limitations of the created model.

For that reason, the distribution of the stresses might indicate the sites with high/low interaction between bone and implant or fusion mass. The stress related to the site should be considered only as an instructive value since the bone material model was assumed as a continuous isotropic material.

LITERATURE

1 Zigler J. E., Anderson P. A., Boden S. D., Bridwell K. H., Vaccaro A. R., *What's new in Spine Surgery*. J. Bone Joint Surgery, vol. 85A, 8, August 2003

2 Benzel E.C., *Spine Surgery: Techniques, Complications, Avoidance, and Management.* Elsevier Churchill Livingstone, 2nd ed., 2005,

ISBN 0–443–06616–07

3 Rothman – Simeone, *The Spine.* W. B. Suanders Comp., 4th ed., 1999, ISBN 0–7216–7176–4

4 White III A. A., Panjabi M. M., *Clinical Biomechanics of the Spine.* Lippincott Williams & Wilkins, 2nd ed., 1990, ISBN 0–397–50720–8

5 Adams M. A., Dolan P., *Spine Biomechanics*. J. Biomech., 38, 2005, pg. 1972–1983

6 Bogduk N., Twomey L. T., *Clinical Anatomy of the Lumbar Spine*, Churchill Livingstone, 1987, ISBN 0–443–03505–9

7 Herzog W., *Clinical Biomechanics – Spinal manipulation.* Churchill Livingstone, 2000, 228 pg. ISBN 0–443–07808–4

8 Adams M. A., Bogduk N., Burton K., Dolan P., Freeman B. J. C., *The Biomechanics of Back Pain.* Churchill Livingstone, 2nd ed., 2006, ISBN–13 978–0–443–10068–0

9 Bernick S., Cailliet R., *Vertebral end–plate changes with aging of human vertebrae.* Spine, 7(2), 1982, pg.97

10 Markolf K. L., Morris J. M., *The Structural Components of the Intervertebral Disc: A Study of their Contributions to the Ability of the Disc to Withstand Compressive Forces.* J. Bone Joint Surg. Am. 56, 1974, pg. 675–687

11 Bogduk N., Macintosh J. E., Pearcy M. J., *A universal model of the lumbar back muscles in the upright position.* Spine, 1992, 17, pg. 897–913

12 Troke M., Moore A. P., Maillardet F. J., Hough A., Cheek E., *A new, comprehensive normative database of lumbar spine ranges of motion.* Clinical Rehabilitation, 2001, 15, pg 371

13 Gertzbein S.D., Holtby R., Tile M., Kapasour A., *Determination of a locus of instantaneous centers of rotation of lumbar disc by Moire Fringes: a new technique.*, Spine, 9, 1984

14 Gertzbein S.D., Seligman J., Holtby R., *Centrode patterns and segmental instability in degenerative disc disease.*, Spine, 10, 1985

15 Dimnet J., Fischer L.P., Carret J.P., *Radiographic studies of lateral flexion in the lumbar spine.*, J. Biomech. 11:143-150, 1978

16 Cossette J.W., Farfan H.F., Robertson G.H., Wells R.V., *The instantaneous center of rotation of the third lumbar intervertebral joint.*, J. Biomech. 4:149, 1971

17 Haberl H., Cripton P. A., Orr T. E., Beutler T., Frei H., Lanksch W. R., Nolte L. P., *Kinematic response of lumbar functional spinal units to axial torsion with and without superimposed compression and flexion/extension.* Eur. Spine J., 2004, 13, pg. 560–566

18 Haher T. R., Bergman M., O'Brien M., Felmly W. T., Choueka J., Welin D., Chow G., Vassiliou A., *The effect of the three columns of the spine on the instantaneous axis of rotation in flexion and extension.* Spine, 16, 1991

19 Tencer A. F., Johnson K. D., *Biomechanics in Orthopedic Trauma: Bone fracture and fixation.* Martin Dunitz Ltd., 1994, ISBN 1–85317–108–5

20 McGill S. M., Yingling V. R., Peach J. P., *Three–dimensional kinematics and trunk muscle myoelectric activity in the eldery spine – a database compared to young people.*, Clin. Biomech., 1999, 14, pg. 389

21 Schultz A., Andersson G., Ortengren R., Haderspeck K., Nachemson A., *Loads on the lumbar spine. Validation of a biomechanical analusis by measurements of intradiscal pressures and myoelectric signals.* J. Bone Joint Surg., 64, 1982

22 Stokes I. A. F., Gardner–Morse M., *Lumbar spinal muscle activation synergies predicted by multi–criteria cost function.* J. Biomech., 34, 2001

23 Patwardhan A. G., Meade K. P., Lee B., *Frontal Plane Model of the Lumbar Spine Subjected to a Follower Load: Implications for Role of Muscles.* J. Biomech. Engineering, 123, June 2001

24 Nussbaum M. A., Chaffin D. B., *Lumbar muscle force estimation using a subject–invariant 5–parameter EMG–based model.* J. Biomech., 31, 1998, pg. 667–672

25 Marras W. S., *Predictions of forces acting upon the lumbar spine under isometric andisokinetic conditions: a model – experiment comparison.* Int. J. Industrial Ergonomics, 3, 1988, pg. 19–27

26 Cholewski J., Simons A. P. D., Radebold A., *Effects of external trunk loads on lumbar spine stability.* J. Biomech., 33, 2000, pg. 1377–1385

27 Arjmand N., Shirazi–Adl A., *Model and in vivo studies on human trunk load partitioning and stability in isometric forward flexions.*, J. Biomech., 39, 2006, pg. 510–521

28 Wang J., Shirazi–Adl A., Parnianpour M., *Search for critical loading condition of the spine – A meta analysis of a nonlinear viscoelastic finite element model.*, Computer Methods in Biomech. And Biomed. Engineering, 8, 2005, pg. 323–330

29 Calisse J., Rohlmann A., Bergmann G., *Estimation of trunk muscle forces using the finite element method and in vivo loads measure by telemeterized internal spinal fixation devices.* J. Biomech., 32, 1999, pg. 727–731

30 Rohlmann A., Claes L. E., Bergmann G., Graichen F., Neef P., Wilke H. J., *Comparison of intradiscal pressures and spinal fixator loads for different body positions and exercises.* Ergonimics, 44, 2001, pg. 781–794

31 Teo E. C., Lee K. K., Ng H. W., Qi, T. X., Yang K., *Determination of load transmission and contact force at facet joints of L2–L3 motion segment using FE method.* J. Musculoskeletal Research, 7, 2, 2003, pg. 97–109

32 Najarin S., Dargahi J., Heidari B., *Biomechanical effect of posterior elements and ligamentous tissues of lumbar spine on load sharing.* Bio–Medical Materials and Engineering, 15, 2005, pg. 145–158

33 Nachemson A., Morris J. M., *In vivo Measurements of Intradiscal Pressure: Discometry, a Method for the Determination of Pressure in the Lower Lumbar Spine.* J of Bone & Joint Sur., 46A, 1964, pg.1077

34 Schultz A., Ortengren R., *Loads on the Lumbar Spine.* J of Bone & Joint Sur.,64A(5), 1982, 713

35 Schultz A. B., *A biomechanical view of scoliosis.* Spine, 1, 1976

36 Belytschko T., Andriacchi T., Schultz A., Galante J., *Analog studies of forces in human spine: computational techniques*., J. Biomech., 6, 1973

37 Panjabi M. M., *Three–dimensional mathematical model of the human spine structure.* J. Biomech., 6, 1973

38 Shirazi–Adl A., Drouin G., *Load–bearing role of facets in a lumbar segment under sagittal plane loadings.* J. Biomech., 20, 1987, pg. 601

39 Deng Y. C., Goldsmith W., *Response of a human head/neck upper–torso replica to dynamic loading. Analytical/numerical model.,* J. Biomech., 20, 1987, pg. 487

40 Nigg B. M., Herzog W. *Biomechanics of the Musculo–Skeletal System.* John Wiley & Sons Ltd., 1999, 2nd ed., ISBN 0–471–97818–3

41 van Deursen D. L., Snijders Ch. J., van Dieën J. H., Kingma I., van Deursen L. L. J. M., *The effect of passive vertebral rotation on pressure in the nucleus pulposus.,* J. Biomech., 34, 2001, pg. 405–408

42 Renner S. M., Natarajan R. N., Patwardhan A. G., Havey R. M., Voronov L. I., Guo B. Y., Andersson G. B. J., An H. S., *Novel model to analyze the effect of a large compressive follower pre–load on range of motions in a lumbar spine.*, J. Biomech., 40, 2007, pg. 1326–1332

43 Wilson D. C., Niosi Ch. A., Zhu Q. A., Oxland T. R., Wilson D. R., *Accuracy and repeatability of a new method for measuring facet loads in the lumbar spine.*, J. Biomech., 2006, 39, pg. 348–353

44 Shirazi–Adl A., *Analysis of large compression loads on lumbar spine in flexion and torsion using a novel wrapping element.*, J. Biomech., 2006, 39, pg. 267–275

45 Rohlmann A., Zander T., Schmidt H., Wilke H.–J., Bergmann G., *Analysis of the influence of disc degeneration on the mechanical behaviour of a lumbar motion segment using the finite element method.*, J. Biomech., 2006, 39, pg. 2484–2490

46 Rohlmann A., Bauer L., Zander T., Bergmann G., Wilke H.–J., *Determination of trunk muscle forces for flexion and extension by using a validated finite element model of the lumbar spine and measured in vivo data.*, J. Biomech., 39, 2006, pg. 981–989

47 Zahn J. M., Sonu R., Vogel H., Crane E., Mazan-Mamczarz K., Rabkin R., Davis R. W., Becker K. G., Owen A. B., Kim S. K., *Transcriptional Profiling of Aging in Human Muscle Reveals a Common Aging Signature.*, PLoS Genetics, Jul2006, Vol. 3 Issue 1

48 Morse C. I., Thom J. M., Birch K. M., Narici M. V., *Changes in triceps surae muscle architecture with sarcopenia.* Acta Physiol. Scand. 2005, 183, pg. 291–298

49 Conley K. E., Esselman P. C., Jubrias S. A., *Ageing, muscle properties and maximal O(2) uptake rate in humans.*, J Physiol, 2000

50 Ascenzi A., Bonuci E., *The compressive properties of single osteons.* Anat. Rec., 161, 1968, pg. 377

51 Clark P., Letts M., *Trauma to the thoracic and lumbar spine in the adolescent.* Canadian Journal of Surgery, vol.44, No.5, October 2001, pg.337–345

52 Gardner A., Grannum S., Porter K., *Thoracic and lumbar spine fractures.* Trauma, 2005, 7, pg 77–85

53 Denis F., *Spinal instability as defined by the three-column spine concept in acute spinal trauma.*, Clin. Orthop., 1984, 189, pg 65–76

54 Aebi M., Thalgott J. S., Webb J. K., *AO ASIF Principles in Spine Surgery.* Springer–Verlag Berlin, 1998, ISBN 3–540–62763–4

55 Holdsworth F., *Review Article Fractures, Dislocations, and Fracture–Dislocations of the Spine.,* J. Bone Joint Surg. Am., 52, 1970, pg. 1534–1551

56 Schneck D. J., Bronzino J. D., *Biomechanics principles and applications.,* CRC Press LLC, 2003, ISBN 0–8493–1492–5

57 Bartel D. L., Davy D. T., Keaveny T. M., *Orthopaedic Biomechanics. Mechanics and Design in Musculoskeletal Systems.,* Pearson Prentice Hall, 2006, ISBN 0–13–008909–5

58 An Y. H., Draughn R. A., *Mechanical Testing of Bone and the Bone–Implant Interface.,* CRC Press LLC, 2000, ISBN 0–8493–0266–8

59 Langton C. M., Njeh C. F., *The Physical Measurement of Bone.*, IOP Publishing Ltd., 2004, ISBN 0–7503–0838–9

60 Schaffler M. B., Burr D. B., *Stiffness of compact bone: effects of porosity and density.,* J.Biomech., 21, 1988

61 Currey J. D., *The relationship between the stiffness and the mineral content of bone.,* J. Biomech., 2, 1969

62 Currey J. D., *The effects of drying and re–wetting on some mechanical properties of cortical bone.,* J. Biomech., 21, 1988

63 Van der Perre G., Lowet G., *Physical meaning of bone mineral content parameters and their relation to mechanical properties.* Clin. Rheumatol., 13, 1994

64 Pattin C. A., Caler W. E., Carter D. R., *Cyclic mechanical property degradation during fatigue loading of cortical bone.* J. Biomech., 29, 1996

65 Fleck C., Eifler D., *Deformation behaviour and damage accumulation of cortical bone specimen from the equine tibia under cyclic loading.,* J.Biomech., 36, 2003

66 Cowin S. C., *Bone poroelasticity.,* J. Biomech., 32, 1999

67 Smit T. H., Huyghe J. M., Cowin S. C., *Estimation of the poroelastic parameters of cortical bone.,* J. Biomech., 35, 2002

68 Pithioux M., Lasaygues P., Chabrand P., *Mechanical properties of orthotropic compact bones using ultrasonic measures.,* XXVI Congres de la Societe de Biomechanique, 2002, pg.92

69 Fyhrie D. P., Kimura J. H., *Cancellous bone biomechanics.,* J. Biomech., 32, 1999

70 Van der Linden J. C., Birkenhäger–Frenkel D. H., Verhaar J. A. N., Weinans H., *Trabecular bone's mechanical properties are affected by its non–uniform mineral distribution.,* J. Biomech., 34, 2001

71 Ulrich D., Van Rietbergen B., Laib A., Rüegsegger P., *The ability of three–dimensional structural indices to reflect mechanical aspects of trabecular bone.,* Bone, 25, 1999

72 Van Rietbergen B., Müller R., Ulrich D., Rüegsegger P., Huiskes R., *Tissue stresses and strain in trabeculae of a canine proximal femur can be quantified from computer reconstructions.,* J. Biomech., 32, 1999

73 Ladd A. J. C., Kinney J. H., *Numerical errors and uncertainties in finite–element modelling of trabecular bone.,* J. Biomech., 31, 1998

74 Morgan E. F., Bayraktar H. H., Keaveny T. M., *Trabecular bone modulus–density relationships depend on anatomic site.,* J. Biomech., 36, 2003

75 Augat P., Link T., Lang T. F., Lin J. C., Majumdar S., Genant H. K., *Anisotropy of the elastic modulus of trabecular bone specimens from different anatomical locations.,* Medical Engineering & Physics, 20, 1998

76 Morgan E. F., Keaveny T. M., *Dependence of yield strain of human trabecular bone on anatomic site.,* J. Biomech., 34, 2001

77 Bayraktar H. H., Morgan E. F., Niebur L., Morris G. E., Wong E. K., Keaveny T. M., *Comparison of the elastic and yield properties of human femoral trabecular and cortical bone tissue.,* J. Biomech., 37, 2004

78 Turner Ch. H., Rho J., Takano Y., Tsui T. Y., Pharr G. M., *The elastic properties of trabecular and cortical bone tissue are similar: results from two microscopic measurement techniques.,* J. Biomech., 32, 1999

79 Frost H. M., *Bone remodelling and its relation to metabolic bone diseases.,* C. Thomas, Springfield, IL, 1973

80 Lee T. C., Staines A., Taylor D., *Bone adaptation to load: microdamage as a stimulus for bone remodelling.,* J. Anat., 2002, 201, pg.437–446

81 Wolff J., *Das Gesetz der Transformation der Knochen.*, Kirchwald, Berlin, 1892

82 Mohsen A., Julian S., Gillespie P., Siddall D. J., Fagan M. J., *Finite element analysis of the lumbar intervertebral disc – a material sensitivity study.*, Proc Inst Mech Eng [H]. 2002; 216(5); pg 299–314

83 Tho B. H., *Development of biomechanical model with individualized geometric and mechanical properties.*, Proc XXIX Congres de la Societe de Biomecanique, Creteil, September 2004

84 Kim H. S., Al–Hassani S. T. S., *A morphological model of vertebral trabecular bone.,* J. Biomech., 35, 2002, pg.: 1101–1114

85 Burstein A. H., Zika J. M., Heiple K. G., Klein L., *Contribution of collagen and mineral to the elastic–plastic properties of bone.*, J. Bone Joint Surg., 57(A), 1975, pg. 956–961

86 Piekarski K., *Fracture of Bone.*, J. AppI. Physics, 41, 1970, pg: 215–223

87 Krag M. H., Beynnon B. D., Pope M. H., *An internal fixator for posterior application to short segments of the thoracic, lumbar, or lumbosacral spine: Design and testing.,* Clin. Orthop., 1986, pg.: 75-98

88 Goel V. K., Kim Y. E., Lim T. H., Weinstein J. N., *An analytical investigation of the mechanics of spinal instrumentation.,* Spine, 1988, pg.: 1003-1011

89 Galante J., Rostoker W., Lueck R., Ray R. D., *Sintered Fiber Metal Composites as a Basis for Attachment of Implants to Bone.,* J. Bone Joint Surg. A, 1971, pg.: 101-114

90 Heck D. A., Nakajima I., Kelly P. J., Chao E. Y., *The effect of load alteration on the biological and biomechanical performance of a titanium fibre-metal segmental prosthesis.,* J. Bone Joint Surg. A, 1986, pg.: 118-126

91 Welsh R. P., Pilliar R. M., Macnab I., *Surgical Implants: The role of surface porosity in fixation to bone and acrylic.,* J. Bone Joint Surg. A, 1971, pg.: 963-977

92 http://www.medtechinsight.com/ReportA307.html

93 http://wwwlib.umi.com/dissertations/preview_page/3225479

94 http://www.spineuniverse.com/displayarticle.php/article1394.html

95 http://www.patentstorm.us/patents/7124067.html

96 http://www.en.wikipedia.org/wiki/image

97 http:// www.orthobiomech.info/surgery.htm

AUTHOR's PUBLICATION

Florian, Z., Wendsche, P., Kotek, V., Kršek, P., Sant, Z.
Stress and strain analysis of degenerated spine element. (*Poster presentation)*
International Conference Biomechanics of Man 2002

Sant Z., Florian Z.
Mechanical properties of the USS lumbar spine implant
Engineering Mechanics, Vol.12, 2005, No.A1, p269-276

Sant Z., Florian Z., Borg J.N., Navrat T
The effect of different loads on the lumbar spine fusion.
Congress of the Czech Society of Biomechanics 2006

Sant Z., Florian Z., Borg J.N.
Biomechanical Analysis of Lumbar Spine Implant
Sixth Malta Medical School Conference 2006

CURRICULUM VITAE

Personal information:

Name and Surname:	Ing. Zdenka SANT
Date of birth:	2nd July 1957
Place of birth:	Brno, Czech Republlic
Nationality:	Czech
Permanent address:	Blazkova 4, 638 00 Brno

Education:

1963 – 1972	Primary & Secondary school in Brno, Czech Republic
1972 – 1976	Mechanical Engineering Technical School in Brno, finishing school with A-levels at the due time
1976 – 1981	Technical University Brno (today BUT) Specialization: Transort Vehicles and Combustion Engines, graduated 1981

Direct Experience:

1981 – 1986	VUEZ Brno (EnergyResearch Institute)
1986 – 1993	VUT Brno, Department of Solid Body Mechanics
1997 – 2001	Department of Mechanical Engineering UoM, part-time
2001	Department of Mechanical Engineering UoM, full-time

Language:

English – active
Russian – passive

ABSTRACT

Stabilita páteře je základním předpokladem zdravého normálního života. Degenerativní procesy společně s úrazy mohou ohrozit normalní funkci páteře, což se projevuje bolestmi zad v lumbární části páteře. Jednou z možných terapií je tzv. fůze páteřního segmentu. Díky fůzi dochází k znehybnění problémového článku páteře a tím i odstranění bolesti. Fůzi páteře je možné docílit operativně a nebo konzervativním přístupem, který je zdlouhavý a pacient je vyřazen na dlouhou dobu z normálního života. Operativní přístup vyžaduje stabilizaci pomocí spinálního fixátoru s užitím kostního štěpu či cementu. V případech operativní léčby je stále poměrně vysoké procento (10 – 15%) případů, kdy nedojde k fůzi a pacient musí podstoupit reoperaci. Fůze je ovlivněna několika faktory, jedním z významných faktorů jsou mechanické poměry v oblasti fůze, které jsou podmíněny vlastnostmi fixatoru. Mechanické vlastnosti fixátoru, které ovlivňují chování článku a silové poměry v dané oblasti, mohou být vyšetřovány ‚in vivo' nebo ‚in vitro'. Jednou z method ‚in vitro' je počítačová simulace chování soustavy. Počítačové modelování vyžaduje vytvoření počítačového modelu na úrovni odpovídající poznatkům doby, hardwarovému a softwarovému vybavení pracoviště.

Na základě analýzy problémů spojených s nedostatečnou fůzí byl navržen postup řešení pomocí počítačového modelování. S předpokladem symmetrie vzhledem k mediální rovině a transversní rovině procházející středem článku, na kterém se fůze provádí, byl vytvořen čtvrtinový model článku. Tento model zahrnuje polovinu obratle L2 s fixátorem složeným z pedikálního šroubu, převlečného zámku, matice a tyče, doplněné o cementový sloupec. Byly vytvořeny dvě varianty cementu, z nichž jedna varianta modeluje ‚obří' výplň síťky ve tvaru elipsy, zatímco druhá varianta modeluje situaci, kdy jsou použity dvě menší válcové výplně síťky. Bylo provedeno porovnání těchto dvou variant tvaru a rozměru cementu a jejich vlivu na důležité mechanické parametry ovlivňující úspěšnou fůzi.

Na základě výsledků řešení bylo konstatováno, že v obou případech mechanické vlastnosti fixátoru podporují fůzi. V případě dvou cementových sloupců relativní pohyb spolu s relativním přetvořením v místě fůze podporuje remodelaci kostní tkáně, zatímco v případě jednotlitého eliptického sloupce bude kostní tkáň vytvářena osifikací tzv. callusu.